doi:10.1016/j.jmb.2010.11.037 J. Mol. Biol. (2011) 405, 653–665

Contents lists available at www.sciencedirect.com

Journal of Molecular Biology

journal homepage: http://ees.elsevier.com.jmb

The Role of MutY Homolog (Myh1) in Controlling the Histone Deacetylase Hst4 in the Fission Yeast *Schizosaccharomyces pombe*

Dau-Yin Chang[1], Guoli Shi[1], Mickaël Durand-Dubief[2], Karl Ekwall[2] and A-Lien Lu[1]*

[1]*Department of Biochemistry and Molecular Biology, School of Medicine, University of Maryland, 108 North Greene Street, Baltimore, MD 21201, USA*
[2]*Department of Biosciences and Nutrition, Center for Biosciences, Karolinska Institutet, Novum, 141 57 Huddinge, Sweden*

Received 20 August 2010; received in revised form 3 November 2010; accepted 16 November 2010
Available online 24 November 2010

Edited by J. Karn

Keywords:
DNA glycosylase;
MYH;
Hst4;
histone deacetylase;
DNA repair

The DNA glycosylase MutY homolog (Myh1) excises adenines misincorporated opposite guanines or 7,8-dihydro-8-oxo-guanines on DNA by base excision repair thereby preventing G:C to T:A mutations. *Schizosaccharomyces pombe* (Sp) Hst4 is an NAD^+-dependent histone/protein deacetylase involved in gene silencing and maintaining genomic integrity. Hst4 regulates deacetylation of histone 3 Lys56 at the entry and exit points of the nucleosome core particle. Here, we demonstrate that the *hst4* mutant is more sensitive to H_2O_2 than wild-type cells. H_2O_2 treatment results in an SpMyh1-dependent decrease in SpHst4 protein level and hyperacetylation of histone 3 Lys56. Furthermore, SpHst4 interacts with SpMyh1 and the cell cycle checkpoint Rad9-Rad1-Hus1 (9-1-1) complex. SpHst4, SpMyh1, and SpHus1 are physically bound to telomeres. Following oxidative stress, there is an increase in the telomeric association of SpMyh1. Conversely, the telomeric association of spHst4 is decreased. Deletion of SpMyh1 strongly abrogated telomeric association of SpHst4 and SpHus1. However, telomeric association of SpMyh1 is enhanced in *hst4*Δ cells in the presence of chronic DNA damage. These results suggest that SpMyh1 repair regulates the functions of SpHst4 and the 9-1-1 complex in maintaining genomic stability.

*Corresponding author. E-mail address: aluchang@umaryland.edu.
Present address: G. Shi, Office of Research, School of Nursing, University of Maryland, 655 West Lombard Street, Baltimore, MD 21201, USA.

Abbreviations used: 9-1-1, Rad9-Rad1-Hus1; ars, autonomously replicating sequence; BER, base excision repair; ChIP, chromatin immunoprecipitation; Clr6, cryptic loci regulator; G^O, 8-oxo-7,8-dihydroguanine; GST, glutathione *S*-transferase; HDAC, histone/protein deacetylase; H3K56, histone H3 Lys56; Hst, homolog of Sir2; MMS, methyl methane sulphonate; Myh1, MutY homolog; qPCR, quantitative PCR; RT, reverse transcription; Sir2, silencing information regulator 2; Sc, *Saccharomyces cerevisiae*; Sp, *Schizosaccharomyces pombe*; Telo, telomere-associated sequences.

0022-2836/$ - see front matter

Introduction

Reactive oxygen species from endogenous and external sources produce thousands of both cytotoxic and mutagenic base lesions and DNA strand breaks per cell per day.[1] The most frequently encountered lesion is 8-oxo-7,8-dihydroguanine (8-oxoG or G^O), which can mispair with adenine during DNA replication and lead to a G:C to T:A transversion.[2,3] In the absence of DNA repair, these events can lead to aging, cancer, and other diseases.[4] Base excision repair (BER) is the major pathway utilized to repair these lesions.[5,6] To initiate BER, DNA glycosylases detect and excise the damaged or incorrectly incorporated bases to generate apurinic/apyrimidinic sites.[7,8] The BER mechanism employed in cellular defense against the 8-oxoG-induced mutagenesis is well conserved among organisms.[2,9]

In the fission yeast *Schizosaccharomyces pombe*, the DNA glycosylase MutY homolog (SpMyh1) removes adenines that are misincorporated opposite to G^O or G,[3,10,11] thus reducing G:C to T:A transversions. Correspondingly, SpMyh1-knockout cells (*myh1*Δ) have a higher mutation frequency than wild-type cells.[12,13] This role of SpMyh1 in mutation avoidance[12] is conserved in the human MutY homolog (hMYH or hMUTYH) (reviewed in Ref. 3). The genomic instability associated with hMYH mutation can lead to MYH-associated polyposis, a hereditary form of colon cancer.[14-18]

Silencing information regulator 2 (Sir2) is a class III NAD^+-dependent histone/protein deacetylase (HDAC) and gene silencer that regulates transcription, recombination, genomic stability, and aging in multiple model organisms.[19,20] Sir2 homologs (sirtuins) are conserved from yeast to mammals.[21-23] The *S. pombe* Sir2 family consists of three members (Sir2, Hst2, and Hst4),[21] whereas mammals encode seven members (SIRT1–SIRT7) (reviewed in Refs. 20,21). *S. pombe* Hst4 (SpHst4) is required for deacetylation of the histone H3 core domain residue Lys56 (H3K56)[24] and several other Lys residues in histone tails.[25] Histone H3K56 acetylation plays important roles in preserving genomic integrity[26,27] and may disrupt histone–DNA interactions at the entry and exit points of the nucleosome core particle.[28] Interestingly, Hst4 represses genes that are involved in amino acid biosynthesis and oxidoreductase activity.[25] SpHst4-defective cells have an elongated cell morphology, chromosomal abbreviations, and a defect in silencing telomeres and centromeres.[24,29] Moreover, *hst4* mutants are more sensitive to many DNA-damaging agents.[24,25,29] These results clearly demonstrate the importance of SpHst4 in maintaining genomic stability.

DNA repair processes are coordinated by cell cycle checkpoint control[30,31] and are controlled by chromatin structure.[32] This coordinated regulation in response to DNA damage increases DNA repair, arrests the cell cycle to allow more time for DNA repair, or triggers apoptosis in cases of extreme DNA damage.[33-36] Rad9, Rad1, and Hus1 are checkpoint sensors that form a heterotrimeric complex (the 9-1-1 complex).[37,38] The sliding clamp structure of the 9-1-1 complex[39-41] shares significant structural homology with proliferating cell nuclear antigen.[42-44] Interestingly, the 9-1-1 complex regulates MYH repair in both *S. pombe* and human cells.[45,46] The role of histone modifications in DNA repair and checkpoint signaling has been previously investigated.[47,48] To study the role of SpHst4 in the repair of oxidative DNA damage and checkpoint signaling, we have investigated whether it functions in the SpMyh1 BER pathway. Here, we demonstrate that SpHst4 interacts with SpMyh1 and the 9-1-1 complex. H_2O_2 treatment results in an SpMYH1-dependent decrease in SpHst4 protein level and hyperacetylation of H3K56. In addition, we show that the telomeric association of SpHst4 and SpMyh1 is dependent on oxidative stress. Significantly, deletion of SpMyh1 strongly abrogated telomeric association of SpHst4 and SpHus1, suggesting that SpMyh1 may act as an adaptor for these proteins. Our results provide new insights into the roles of DNA repair, histone acetylation, and checkpoint regulation in the maintenance of genomic stability.

Results

Hst4-defective cells are more sensitive to hydrogen peroxide

S. pombe Hst4 plays a critical role in preserving genomic integrity.[24,25,29] *hst4* mutants have been shown to be more sensitive to hydroxyurea, phleomycin, UV light, methyl methane sulphonate (MMS), and the microtubule-destabilizing agent tiabendazole than wild-type cells.[24,25,29] However, its sensitivity to oxidative stress has not been demonstrated. In Fig. 1a, we showed that *hst4* mutant cells were more sensitive to H_2O_2 than wild-type cells. H_2O_2 sensitivity was observed for concentrations higher than 1 mM. We also tested two additional *S. pombe* mutants lacking the histone deacetylases Clr6 and Sir2. Clr6 (cryptic loci regulator) is a class I HDAC involved in epigenetic regulation,[49] and Sir2 belongs to the same class III HDAC family as Hst4.[29,50] As shown in Fig. 1b, *clr6*Δ was as sensitive to 2 mM H_2O_2 as the *hst4*Δ mutant; however, *sir2*Δ did not show an increase in H_2O_2 sensitivity.

Oxidative damage alters SpHst4 expression and histone H3K56 acetylation

To determine whether the SpHst4 protein level is altered after oxidative stress, we prepared total cell extracts from a strain expressing Myc-tagged

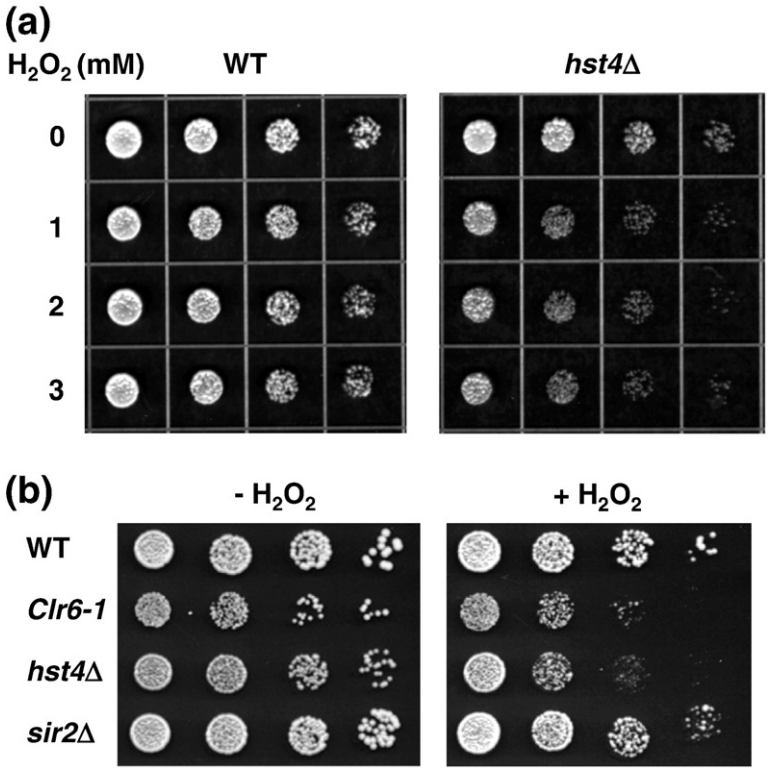

Fig. 1. *S. pombe hst4*Δ cells are more sensitive to H_2O_2. (a) Wild-type (WT) and *hst4*Δ *S. pombe* cells in exponential growth were treated with 0, 1, 2, and 3 mM H_2O_2 for 30 min and diluted for every 4-fold, and 4 μl was spotted onto YES plates. (b) Wild-type (WT) cells and three HDAC mutants *clr6*Δ, *hst4*Δ, and *sir2*Δ were treated with or without 2 mM of H_2O_2 for 30 min and diluted for every 5-fold, and 4 μl was spotted onto YES plates.

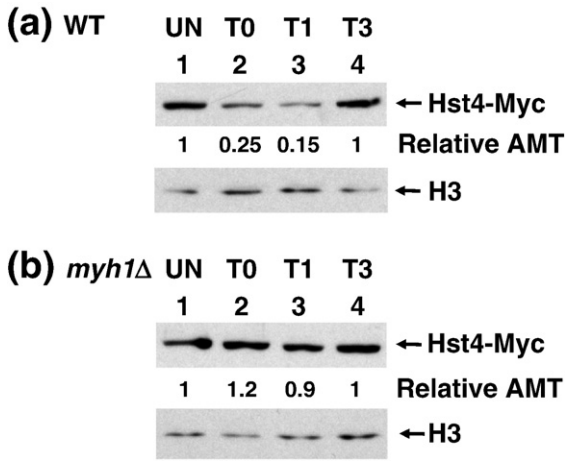

Fig. 2. SpHst4 protein level decreases following H_2O_2 treatment in wild-type (WT) but not in *myh1*Δ cells. *S. pombe* Hu1500 (a) and Hst4-MYC *myh1*Δ (b) were treated with 5 mM H_2O_2 for 30 min and then recovered for 0 h (T0), 1 h (T1), or 3 h (T3) or remained untreated (UN). Total cell extracts were prepared, separated on 4–20% gradient SDS-polyacrylamide gels, and subjected to Western blotting with a mixture of antibodies against c-Myc and histone H3. The amounts of SpHst4-Myc were quantitated relative to those of H3 (Relative AMT).

SpHst4 and monitored the SpHst4 protein by Western blotting with c-Myc antibody (Fig. 2). The SpHst4 protein levels were normalized to the amounts of histone H3. Upon treatment with 5 mM H_2O_2 for 30 min, the level of SpHst4 decreased by 4-fold (Fig. 2a, lane 2, upper panel). The level of SpHst4 continued to decrease by 7-fold after recovery in H_2O_2-free medium for 1 h (Fig. 2a, lane 3, upper panel) but returned to normal level after a 3-h recovery (Fig. 2a, lane 4, upper panel). Because SpHst4 controls the acetylation of histone H3K56,[24] the decreased level of SpHst4 observed after treatment with H_2O_2 may contribute to the up-regulation of H3K56 acetylation. To test this, we monitored the acetylation level of H3K56. In wild-type cells, the acetylation of H3K56 increased immediately after H_2O_2 treatment (Fig. 3, lane 2, upper panel) and then continued to increase during the first 3 h of the recovery period (Fig. 3, lanes 3 and 4, upper panel). The level of H3K56 acetylation was very high in untreated *hst4* cells (Fig. 3, lane 5, upper panel). This observation is consistent with the finding that Hst4 can deacetylate H3K56.[24] However, the level of H3K56 acetylation in *hst4* cells did not change significantly after H_2O_2 treatment (Fig. 3, lanes 5–8, upper panel).

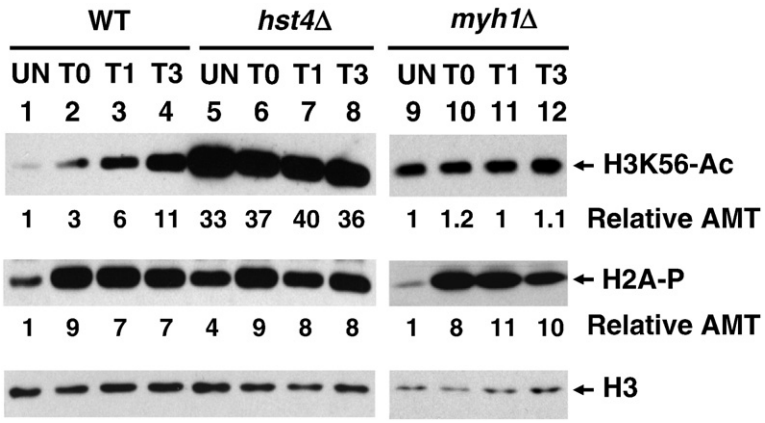

Fig. 3. The levels of acetylated H3K56 (H3K56-Ac) and phosphorylated H2A (H2A-P) increase following H_2O_2 treatment in WT cells. *S. pombe* Hu303, Hu1481 (*hst4*Δ), and JSP303-Y4 (*myh1*Δ) were treated with 5 mM H_2O_2 for 30 min and then recovered for 0 h (T0), 1 h (T1), or 3 h (T3) or remained untreated (UN). Total cell extracts were prepared and separated into two sets of 15% SDS-polyacrylamide gels. Set 1 gel was subjected to Western analysis with H3K56Ac antibody. The membrane was then stripped and probed with H2A-P antibody. Set 2 gel was subjected to Western analysis with H3 antibody. Lanes 1–8 are on the same membrane, while lanes 9–12 are on separate membranes and Western blotting was performed separately. The amounts of H3K56Ac and H2A-P were quantitated relative to those of H3 (Relative AMT).

Because *S. pombe* Hst4 is important in DNA repair and genomic stability[24,25,29] and *hst4* mutants are more sensitive to H_2O_2, we asked whether the changes in SpHst4 protein levels were dependent on SpMyh1. As shown in Fig. 2b, the SpHst4 protein levels were not altered in *myh1*Δ cells following H_2O_2 treatment. Consistent with the finding that SpHst4 can regulate H3K56 acetylation, the H3K56 acetylation levels were not altered in *myh1*Δ cells following H_2O_2 treatment (Fig. 3, lanes 9–12, upper panel).

To determine whether the decreased SpHst4 protein level following H_2O_2 treatment is controlled at the level of transcription, we examined the *hst4* mRNA level. As shown in Table 1, using *act1* as a control and reverse transcription quantitative PCR (RT-qPCR) analysis, the *hst4* mRNA level of H_2O_2-treated wild-type (Hu1500) cells is 1.08-fold that of the untreated cells, while the *hst4* mRNA level of H_2O_2-treated *myh1*Δ cells is 0.91-fold that of the untreated cells. Thus, the level of *hst4* mRNA was altered neither in wild-type cells nor in *myh1*Δ cells following 1-h recovery after treatment with H_2O_2. Therefore, the decreased SpHst4 protein level observed was not the result of *hst4* mRNA transcriptional inhibition.

Table 1. The mRNA level of *hst4*$^+$ does not change following H_2O_2 treatment and is independent of SpMyh1

		Ct				
		hst4$^+$	*Act1*$^+$	ΔCt	Fold[a]	Fold[b]
Hu1500	UN	20.01	15.07	5.04		
Hu1500	T1	20.22	15.28	4.94	1.07	1.08 ± 0.05
*myh1*Δ	UN	20.22	14.72	5.50		
*myh1*Δ	T1	20.09	14.68	5.41	1.06	0.91 ± 0.20

[a] Cells at an OD_{600} of 0.8 were exposed to 5 mM H_2O_2 for 30 min and recovered for 1 h (T1) or left untreated (UN). RNA was prepared and RT-qPCR was performed with primers specific for *hst4*$^+$ and *act1*$^+$. The amount of *hst4*$^+$ mRNA was quantitated relative to that of *act1*$^+$. Fold changes of T1 relative to UN are presented.

[b] Average of three separate experiments, with errors reported as SDs.

Oxidative damage stimulates histone H2A phosphorylation

Mammalian ATR and ATM checkpoint kinases modulate chromatin structures near DNA breaks by phosphorylating histone H2AX.[51] *S. pombe* H2A is similarly phosphorylated following ionizing radiation by the ATR/ATM-related kinases Rad3 and Tel1.[52] The phosphorylated forms of human H2AX and *S. pombe* H2A are thought to be important for DNA repair and checkpoint maintenance. To check whether H2A is phosphorylated following oxidative stress, we monitored H2A phosphorylation in wild-type, *hst4*Δ, and *myh1*Δ cells following H_2O_2 treatment. In wild-type and *myh1*Δ cells, H2A phosphorylation increased approximately 8-fold immediately after H_2O_2 treatment and remained high during the next 3 h as the cells recovered (Fig. 3, lanes 1–4 and lanes 9–12, middle panel). Thus, H2A phosphorylation in response to oxidative damage is independent of SpMyh1. The result is consistent with the previous finding that H2A phosphorylation occurs at double-strand breaks induced by oxidative stress.[52,53] In untreated *hst4*Δ cells, the level of H2A phosphorylation was higher than that in wild-type cells (Fig. 3, compare lanes 1 and 5, middle panel). This result suggests that the DNA damage checkpoint is

activated in *hst4*Δ cells and is consistent with previous reports that *hst4*Δ cells contain DNA damage[24,29] and elevated levels of Chk1 phosphorylation.[24] In H_2O_2 treated *hst4Δ* cells, the level of H2A phosphorylation was 2-fold higher than that in untreated *hst4Δ* cells (Fig. 3, lanes 5–8, middle panel) and was comparable to H2O2-treated wild-type cells (Fig. 3, compare lanes 2–4 with lanes 6–8, middle panel).

SpHst4 interacts with SpMyh1 and the Rad9-Rad1-Hus1 (9-1-1) complex

Because the change in SpHst4 protein levels following oxidative stress is dependent on SpMyh1, we asked whether SpHst4 interacts with SpMyh1 DNA glycosylase. We demonstrated that SpHst4 physically interacted with SpMyh1 by glutathione *S*-transferase (GST) pull-down (Fig. 4a) and coimmunoprecipitation (Fig. 4b). Treatment with H_2O_2 resulted in approximately 3-fold increased SpHst4–SpMYH1 interaction (Fig. 4b, compare lanes 2 and 4).

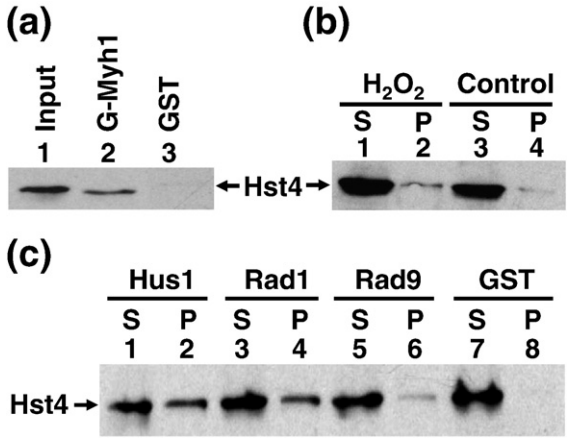

Fig. 4. SpHst4 interacts with SpMyh1 and the Rad9/Rad1/Hus1 subunits. (a) Pull-down of SpHst4 by GST-SpMyh1. GST-SpMyh1 (lane 2) and GST alone (lane 3) were immobilized onto glutathione–Sepharose and incubated with extracts from Hu1500 containing SpHst4-Myc. The pellets were fractionated by 10% SDS-PAGE followed by Western blot analysis with c-Myc antibody. Lane 1 contains 10% of the input yeast extracts. (b) The interaction of SpHst4 and SpMyh1 was enhanced following oxidative stress. Hu1500 cells were exposed to 5 mM H_2O_2 for 30 min and recovered for 1 h or left untreated (control). Total soluble cell extracts were prepared and analyzed by immunoprecipitation with antibody against SpMyh1. Western blotting was performed to detect SpHst4. S, supernatant; P, pellet. (c) Pull-down of SpHst4 by GST-SpHus1, GST-SpRad1, and GST-SpRad9. GST-SpHus1 (lanes 1 and 2), GST-SpRad1 (lanes 3 and 4), GST-SpRad9 (lanes 5 and 6), and GST alone (lanes 7 and 8) were immobilized onto glutathione–Sepharose and incubated with purified SpHst4-Myc. The supernatants (10%) and pellets were fractionated by 10% SDS-PAGE followed by Western blot analysis with c-Myc antibody.

It has been shown that SpHst4 functions in the DNA damage response pathway.[24] Moreover, several checkpoint components are essential for the survival of the *hst4*Δ mutant.[24] We have shown that MYH glycosylase is associated with the 9-1-1 complex in both *S. pombe* and human cells.[45,46] Because SpHst4 interacts with SpMyh1, we asked whether SpHst4 interacts with the 9-1-1 complex. We demonstrated that purified SpHst4 interacted with all three subunits of the 9-1-1 complex (Fig. 4c). The interaction of SpHst4 with SpHus1 and SpRad1 was stronger than the SpHst4–SpRad9 interaction. These results suggest that SpHst4 and SpMyh1 form a complex with the 9-1-1 complex and that SpHst4 may have a direct role in BER and DNA damage response.

SpHst4 and SpMyh1 are bound to telomeric DNA

There is increasing evidence that supports the importance of regulating DNA repair at telomeres.[54] Oxidative damage to CG-rich telomeric DNA requires efficient BER to maintain its integrity.[55,56] The *S. pombe* telomeres of chromosomes I and II are ~300 bp in length with variable repeat unit of consensus $T_{1\text{-}3}AC_{0\text{-}1}A_{0\text{-}2}C_{0\text{-}1}G_{1\text{-}8}$, and TTACAGG is the most common repeat. The telomeres of chromosome III of *S. pombe* consist of ~150 rDNA repeats separated into two clusters at both ends. One rDNA repeat (~10.5 kb) consists of a transcription unit for the 35S rRNA precursor and a nontranscribed sequence, which contains an autonomously replicating sequence (ars) element (ars3001) and a replication fork barrier.[57] A recent report has shown that SpHst4 binds to over 300 open reading frames and heterochromatin regions including *mat*, rDNA, and telomeres.[25]

We have confirmed that SpHst4 is physically bound to telomeres by performing a chromatin immunoprecipitation (ChIP) assay with *S. pombe* expressing Myc-tagged SpHst4 (Fig. 5a). Precipitated DNA was quantitated by qPCR with primers for the telomere-associated sequences (Telo). Telomeric DNA was specifically enriched 8-fold from Hst4-Myc immunoprecipitant, and the association of SpHst4 at telomeres was 7-fold over that at the *ade6* region (Fig. 5a, columns 1 and 2). Further ChIP analyses of rDNA regions (17S, replication fork barrier, and ars3001) and non-telomere-adjacent regions (ars2004 and ars3005) indicated that SpHst4 was also enriched at ars3001 but not at the other tested sites (Fig. 5a). The association of SpHst4 at ars3001 was 4-fold over that at the *ade6* region (Fig. 5a, columns 2 and 5).

The ChIP assay with SpMyh1 polyclonal antibody demonstrated that SpMyh1 was also enriched at telomeres of chromosomes I and II as well as at the ars3001 region (Fig. 5b, columns 1 and 5) but not at the other tested sites (Fig. 5b). The associations of

SpMyh1 at telomeres and ars3001 were about 4.5-fold over that at the *ade6* region. Interestingly, the pattern of SpMyh1 association with telomeres is similar to that of SpHst4.

The recruitment of SpMyh1 and SpHst4 to telomeres is altered by oxidative stress

Because both *myh1*- and *hst4*-defective cells are more sensitive to H_2O_2 (Fig. 1),[12] we tested whether their association at the telomeres was affected by oxidative stress. Fig. 5c indicated that the association of SpHst4 at telomeres decreased by 45% when *S. pombe* cells were treated with H_2O_2 and then recovered for 1 h (Fig. 5c, column 1 *versus* column 2).

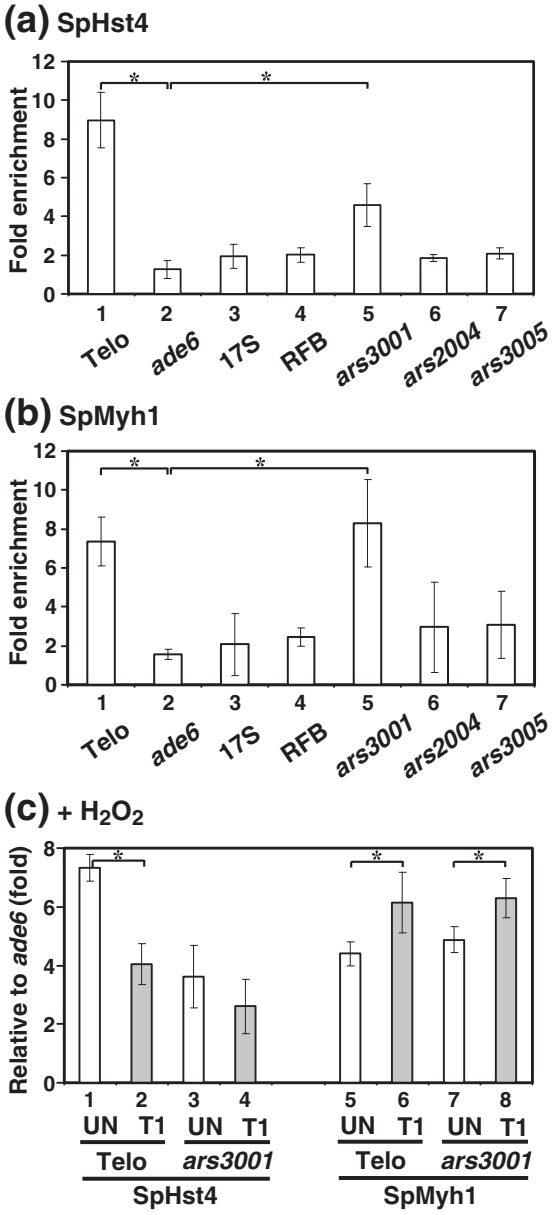

This result is consistent with Fig. 2a, which shows that the total SpHst4 protein level decreased by 85%. We have reported that SpMyh1 protein levels remain unchanged following H_2O_2 treatment.[45] However, the association of SpMyh1 at telomeres increased by 40% in oxidatively damaged *S. pombe* cells (Fig. 5c, column 5 *versus* column 6). The changes in the association of SpHst4 and SpMyh1 at ars3001 were similar to their association at telomeres of chromosomes I and II but were less significant when *S. pombe* cells were treated with H_2O_2 (Fig. 5c, columns 3, 4, 7, and 8).

SpHst4 and SpHus1 association at telomeres is substantially dependent on SpMyh1

The correlated association of SpHst4 and SpMyh1 at telomeres and ars3001 (Fig. 5a and b) prompted us to investigate their mutual dependence. First, we examined whether the recruitment of SpHst4 to telomeres was dependent on SpMyh1. Using ChIP assay with c-Myc antibody, we showed that deletion of SpMyh1 abrogated SpHst4 association to telomeres (Fig. 6a, compare columns 1 and 2, and columns 3 and 4). In untreated cells, the association of SpHst4 at telomeres reduced from 7-fold in wild-type cells to 2-fold in *myh1*Δ cells. In H_2O_2-treated cells, the association of SpHst4 at telomeres reduced from 4-fold in wild-type cells to basal level in *myh1*Δ cells. As a control, the enrichment of SpMyh1 to telomeres was lost in the *myh1*Δ mutant (Fig. 6a, compare columns 5 and 6, and columns 7 and 8). Thus, SpHst4 association at telomeres is dependent on SpMyh1.

The *S. pombe* 9-1-1 complex has been shown to associate with telomeres and is important in

Fig. 5. The associations of SpHst4 and SpMyh1 at telomeres and ars3001 of the rDNA repeat are altered following oxidative stress. (a) *S. pombe* cells (Hu1500) were subjected to ChIP assay with c-Myc antibody to precipitate SpHst4-Myc-associated DNA. Precipitated DNA (IP) samples were amplified with the primers listed in Table S2 by qPCR. Enrichment (*n*-fold) was calculated according to the formula $2^{\Delta Ct - \Delta CtControl}$, in which ΔCt is the difference between the number of cycles required to go above background in input and IP samples. The control is the sample with beads only. Statistical significances between telomeres (Telo) and ars3001 relative to *ade6*$^+$ are indicated with stars. (b) ChIP was performed similarly to (a) except that SpMyh1 antibody was used to precipitate SpMyh1-associated DNA. (c) ChIP was performed similarly to (a) and (b) except that Hu1500 cells were treated with 5 mM H_2O_2 for 30 min and then recovered for 1 h (T1) or left untreated (UN). c-Myc antibody (columns 1–4) and SpMyh1 antibody (columns 5–8) were used to precipitate SpHst4- and SpMyh1-associated DNA, respectively. Fold enrichment at Telo and ars3001 was calculated relative to *ade6*$^+$. Statistical significance ($P<0.02$) between wild-type and *hst4*Δ is indicated with a star.

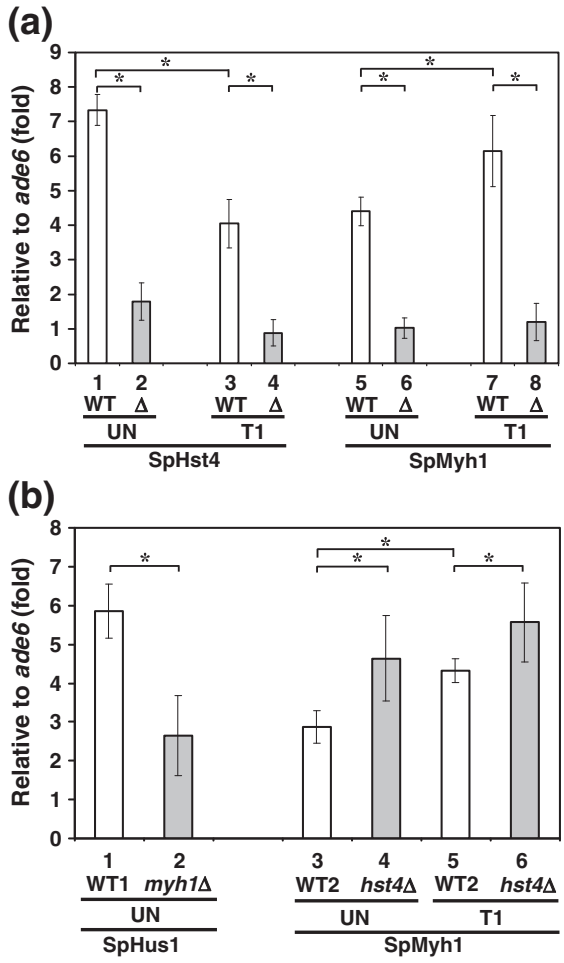

Fig. 6. The association of SpHus1 and SpHst4 to telomeres is dependent on SpMyh1, and the association of SpMyh1 to telomeres is enhanced in *hst4*Δ cells. (a) ChIP was performed similarly to Fig. 5 except that both Hu1500 (WT) and Hst4-MYC *myh1*Δ (Δ) cells were used. Cells were treated with 5 mM H_2O_2 for 30 min and then recovered for 1 h (T1) or left untreated (UN). c-Myc antibody (columns 1–4) and SpMyh1 antibody (columns 5–8) were used to precipitate SpHst4- and SpMyh1-associated DNA, respectively. Fold enrichment at Telo was calculated relative to *ade6*$^+$. Statistical significance between wild-type and *myh1*Δ is indicated with a star. (b) ChIP was performed similarly to (a) except that Hus1-MYC (WT1), Hus1-MYC *myh1*Δ (*myh1*Δ), Hu303 (WT2), and Hu1481 (*hst4*Δ) cells were used. c-Myc antibody (columns 1–2) and SpMyh1 antibody (columns 3–6) were used to precipitate SpHus1- and SpMyh1-associated DNA, respectively. Fold enrichment at Telo was calculated relative to *ade6*$^+$. Statistical significance ($P<0.02$) between wild-type and *hst4*Δ is indicated with a star.

telomere maintenance.[58,59] Since SpHst4 and SpMyh1 form a complex with the 9-1-1 complex, we examined whether the recruitment of SpHus1 to telomeres is dependent on SpMyh1. Myc-SpHus1 was particularly enriched at telomeres of chromosomes I and II (Fig. 6b, column 1), confirming a previous report.[59] Deletion of SpMyh1 strongly abrogated but did not completely prevent SpHus1 association to telomeres (Fig. 6b, compare columns 1 and 2), suggesting the possible involvement of other factors for SpHus1 association at telomeres.

SpMyh1 association at telomeres is enhanced in *hst4*Δ cells

Next, we examined whether the recruitment of SpMyh1 at telomeres was dependent on SpHst4. As shown in Fig. 6b (lanes 3–6), the association of SpMyh1 at telomeres was increased either in the untreated or H_2O_2-treated *hst4*Δ cells. This result is in agreement with the finding that the untreated *hst4*Δ cells contain DNA damage, which is indicated by elevated levels of H2A phosphorylation (Fig. 3, lane 5, middle panel) and Chk1 phosphorylation.[24] This increased DNA damage may lead to enhanced association of SpMyh1 with telomeres.

Discussion

S. pombe Hst4, a member of the class III HDACs (sirtuins), plays an important role in maintaining genomic stability.[24,25,29] Sirtuins are gene silencers/regulators that impact the aging process (reviewed in Refs. 20,21,60). *S. pombe hst4* mutants are more sensitive to many DNA-damaging agents[24,25,29] including H_2O_2 (Fig. 1). *S. pombe hst4* mutants have constitutively elevated levels of H3K56 acetylation following treatment with both H_2O_2 (Fig. 3) and methylating agents.[24] In this study, we show that SpHst4 interacts with SpMyh1 DNA glycosylase and the 9-1-1 checkpoint sensor. Moreover, Myh1 is required for SpHst4 association at the telomeres, the decrease in SpHst4 protein level, and hyperacetylation of histone H3K56 following oxidative stress. Thus, SpMyh1 repair is correlated with SpHst4-mediated histone modification. Mammalian sirtuins play a role in many biological processes, such as insulin secretion, fat mobilization, response to stress, and lifespan regulation.[19,20] Particularly, *sirt6*-knockout mice display premature aging.[61,62] Similar to *S. pombe hst4* mutants, SIRT6-deficient cells are more sensitive to DNA-damaging agents (methylating agents, H_2O_2, and ionizing radiation) and have an increased frequency of genomic aberrations.[62] Moreover, SIRT6 has a function in modulating telomeric chromatin.[63] Furthermore, SIRT6 and SpHst4 share similar substrate specificity on H3K9 and H3K56.[24,25,63-65] Most importantly, it has been shown that SIRT6 plays a role in BER because expression of DNA polymerase β in SIRT6-deficient cells restores resistance to DNA-damaging agents.[61,62] Based on the similar phenotypes of Hst4-defective *S. pombe* cells and *sirt6*-knockout mice[62]

and their roles in histone deacetylation and BER, we hypothesize that SpHst4 may be the functional homolog of mammalian SIRT6.

Telomeres contain DNA double-strand ends that do not trigger the DNA damage response; nevertheless, they require DNA repair and checkpoint proteins for maintenance. The CG-rich telomere sequence is particularly susceptible to oxidative damage.[66-68] Oxidative damage is repaired inefficiently in telomeric DNA in comparison to the rest of the chromosome.[68] Single and multiple G^O lesions in the human tandem telomeric sequence repeats disrupt recognition by the telomere repeat binding factors TRF1 and TRF2.[69] TRF2 has been shown to interact with enzymes involved in BER (DNA polymerase β and FEN-1).[55] Furthermore, OGG1 DNA glycosylase is involved in repairing G^O lesions in telomeres.[56] We hypothesize that Myh1, Hst4, and the 9-1-1 complex are involved in the reduction of G:C to T:A transversions at the telomeres based on the following results. First, both *myh1* and *hst4* mutants are more sensitive to H_2O_2 (Fig. 1).[12] Second, Hst4 interacts with Myh1 and the 9-1-1 complex (Fig. 4), and Myh1 interacts with the 9-1-1 complex.[46] Third, Myh1, Hst4, and the 9-1-1 complex are enriched at telomeres (Figs. 5 and 6).[25,58,59] The association of SpMyh1 at telomeres and ars3001 (Fig. 5b) is a new and interesting finding and indicates that SpMyh1 is enriched at certain defined sites of the genome. The telomeric presence of SpMyh1 likely indicates that it plays a role in maintaining the CG-rich regions. When telomeres are damaged, Myh1 recognizes the A/G^O mismatch and recruits SpHst4 and the 9-1-1 complex for efficient repair (Figs. 4 and 6). However, further investigation is necessary to determine the biological significance of SpMyh1 enrichment at ars3001. It appears that SpMYH1 association at ars3001 is not related to replication origin because SpMYH1 does not bind to all autonomously replicating sequences such as ars2004 and ars3005.

It has been shown that SpHst4 can deacetylate H3K56 and histone tails.[24,25] Sufficient data support that a balanced level of H3K56 acetylation is critical for genome integrity. Unacetylatable histone H3 (H3K56R), complete loss of H3K56 acetylation (*Rtt109* deletion), acetylation mimic H3K56Q mutant, and H3K56 hyperacetylation in the *hst4* mutant (or *hst3 hst4* double mutant in *Saccharomyces cerevisiae*) all elicit similar phenotypes that exhibit sensitivity to DNA-damaging agents.[24,70-74] Recent studies proposed a model showing that H3K56 acetylation plays a role in replication-coupled chromatin assembly and chromatin reassembly during double-strand break repair and checkpoint recovery.[75,76] H3K56 acetylation is enriched on chromatin fractions undergoing DNA repair and has been proposed to open chromatin for DNA repair.[77] Our results support the notion that DNA damage alters H3K56 acetylation. We have shown that when wild-type *S. pombe* cells are treated with H_2O_2 with a 1-h recovery, the H3K56 acetylation is up-regulated via down-regulation of SpHst4 (Figs. 2 and 3), and SpHst4 association at the telomeres is reduced (Fig. 5c). However, after 3 h of recovery, the Hst4 protein level is restored, but the H3K56 acetylation level is increased. It is possible that a histone acetyltransferase (such as Rtt109)[74] may be activated, other histone deacetylases may be reduced, or Hst4 deacetylase activity may be inhibited. Because SpMyh1 repairs replication errors, its repair is coupled with DNA replication through interaction with proliferating cell nuclear antigen.[78] Interestingly, acetylation of H3K56 occurs during S phase.[24,70,74] Thus, SpMyh1 repair may occur before deposition of newly assembled nucleosomes.

It has been shown that loss of ScHst3-mediated regulation of H3K56 acetylation in *S. cerevisiae* results in a defect in the S-phase DNA damage checkpoint, and that the increased level of H3K56 acetylation is accomplished by SpHst4 down-regulation in response to the methylating agent MMS.[24,73] In *S. cerevisiae*, ScHst3 undergoes rapid ScMec1-dependent phosphorylation and is targeted for ubiquitin-mediated proteolysis following MMS treatment.[24,73] We have shown that down-regulation of SpHst4 following H_2O_2 treatment is not accompanied by down-regulation of *hst4* mRNA. Thus, the mechanism of regulating SpHst4 expression level following oxidative stress may follow a similar mechanism as ScHst3 by MMS treatment.[24,73] Our results indicate that Myh1 is required for SpHst4 association at the telomeres, the decrease in SpHst4 protein level, and hyperacetylation of histone H3K56 following oxidative stress. Therefore, we propose that by recruiting SpHst4 to mismatched DNA sites, SpMyh1 may expose Hst4 protein to targeted degradation by the activated DNA damage checkpoint. Targeted H3K56 acetylation could facilitate DNA repair by creating a more open chromatin or by recruiting DNA damage signaling proteins.[73] The direct physical interactions of SpHst4 with SpMyh1 and the 9-1-1 complex support this notion. Thus, the increased genomic instability in *hst4*Δ with global overacetylation of H3K56 or *Rtt109*Δ without H3K56 acetylation may be caused by the inability to mark H3K56 on the chromatin containing damaged or mismatched DNA.

Hst4-defective *S. pombe* cells have elevated chromosome abbreviation and DNA damage.[24,25,29] Our data (Fig. 6b) are consistent with the idea that the association of SpMyh1 at telomeres is increased in order to repair DNA damage in *hst4*Δ cells. Moreover, the interaction of SpHst4 with the 9-1-1 complex links histone acetylation with checkpoint regulation. It has been shown that several checkpoint components are essential for the survival of *hst4*Δ mutant.[24] In addition, Celic *et al.*[79] have

observed that the temperature-sensitive phenotype of *S. cerevisiae hst3 hst4* can be suppressed by inactivation of the 9-1-1 complex. In conclusion, our results suggest that SpMyh1 repair coupled with cell cycle checkpoint and histone acetylation is critical for genomic stability and/or telomere maintenance.

Materials and Methods

Yeast *S. pombe* strains and growth

The yeast strains used in this study are listed in Table S1. Standard procedures and media were used for culture growth, transformation, and genetic analysis.[80] Yeast cells were grown in YES medium (5 g of yeast extract, 30 g of glucose, and 100 mg each of adenine, histidine, leucine, lysine, and uracil per liter) for regular maintenance. The Hu1500 strain was constructed by epitope tagging of the endogenous *hst4*$^+$ gene, using a previously described procedure.[81] The protein was tagged at the C terminus with 6xMyc (i.e., natural promoter and expression levels). The *myh1*Δ mutant containing *hst4*$^+$-Myc was constructed by two genetic crosses. The marker *his3D1* from FY526 was introduced to Hu1500, and then the resulting strain was crossed with JSP303-Y4 (*myh1*Δ::*his3*$^+$) to generate the Hst4-MYC *myh1*Δ strain. Both strains were verified by PCR for correct integration and by Western blotting for expression of Hst4-MYC.

H_2O_2 treatment of yeast cells

For H_2O_2 sensitivity, 1 ml of an overnight yeast culture grown in YES was added to 20 ml of YES medium. At an OD_{600} of 0.5, 2 ml of the culture was aliquoted into each 30-ml test tube, and hydrogen peroxide was added to each culture at various concentrations. After incubating for 30 min, the cells were spun down and resuspended in peroxide-free fresh medium. Diluted cells (4 μl) were spotted onto YES plates. The plates were placed in a 30 °C incubator for 2–3 days. For cell extract and mRNA preparations, cells at an OD_{600} of 0.6–0.8 were exposed to 5 mM H_2O_2 for 30 min and recovered for different time intervals or left untreated (control).

Preparation of cell extracts and Western blotting

Total cell extracts were prepared from 10 ml of *S. pombe* culture. The cells were washed with 20% TCA and frozen at −80 °C. The cell pellet was thawed and resuspended in 0.25 ml of 20% TCA and lysed by glass beads. After precipitation with 5% TCA, the pellet was washed with 0.75 ml of ethanol and resuspended in 40 μl of 1 M Tri–HCl (pH 8.0). After adding 80 μl of 2× SDS loading buffer, the solution was boiled for 10 min and then centrifuged at 14,000 rpm for 5 min. The supernatants were collected and portions were fractionated on a 15% SDS-polyacrylamide gel for histones or 4–20% gradient gel for SpHst4-Myc. The proteins were transferred onto a nitrocellulose membrane. Western blot analyses were performed with antibodies against c-Myc tag (Santa Cruz Biotechnology), H3 (Abcam), K56 acetylated H3 (Active Motif), S129 phosphorylated H2A (Abcam), and tubulin (Abcam). Soluble cell extracts were prepared as described by Chang *et al.*,[12] except without ammonium sulphate precipitation.

Preparation of RNA and RT-PCR

S. pombe cells were grown to log phase, treated with 5 mM H_2O_2 for 30 min, and then recovered for 1 h (T1) in fresh YES medium or left untreated. Total RNA was isolated with acid phenol procedures[82] and further cleaned up with RNeasy Mini Kit (Qiagen). The RNA (100 ng) was used as a template for RT-qPCR reactions using primers for *hst4* and *act1* (see Table S2) and iScript one-step RT-PCR kit with SYBR Green SuperMix (Bio-Rad). The reactions were carried out with Roche Light-Cyler 480 at 50 °C for 10 min and 95 °C for 5 min for RT and then followed by PCR cycles (95 °C for 30 s, 55 °C for 30 s, and 70 °C for 1 min). The mRNA level of *hst4* was calculated relative to that of *act1* as ΔCt, which is the difference between the number of cycles required to go above background in *hst4* and *act1* samples. The fold difference of *hst4* mRNA levels of treated cells over untreated cells (un) is calculated according to the formula $2^{\Delta Ct(un) - \Delta Ct(T1)}$. The reactions were carried out in duplicate and data were averaged from three independent experiments.

Cloning, expression, and purification of SpHst4

The cDNA of SpHst4 was amplified by PCR from an *S. pombe* cDNA library in pGADGH (kindly provided by D. Beach, Cold Spring Harbor Laboratory) using Pfu DNA polymerase (Stratagene) with the appropriate primers (listed in Table S2). The PCR products were digested with BamHI and SalI, cloned into pET21a (BamH1 and Xho1 digested), transformed into *Escherichia coli* DH5α cells (Invitrogen), and selected via ampicillin resistance. All clones were confirmed by DNA sequencing.

To express the His-tagged SpHst4 protein, the plasmid was transformed into Rosetta cells (Invitrogen). The cells were cultured in Luria-Bertani broth containing 100 μg/ml ampicillin and 35 μg/ml chloramphenicol at 37 °C. Protein expression was induced at an A_{590} of 0.6 by the addition of isopropyl 1-thio-β-D-galactopyranoside to a final concentration of 0.4 mM. After 16 h at 25 °C, the cells were harvested by centrifugation at 10,000*g* for 20 min. The SpHst4-His protein was purified by Ni–NTA resin (Qiagen) under native conditions according to the manufacturer's protocol. The SpHst4-His protein was dialyzed twice with 1 liter of TEG buffer [50 mM Tris–HCl (pH 7.4), 0.1 mM EDTA (ethylenediaminetetraacetic acid), 50 mM KCl, 10% glycerol, 0.5 mM dithiothreitol, and 0.1 mM PMSF] and further purified by two connected 1-ml SP columns (GE Health) equilibrated with TEG buffer. Upon washing with 12 ml of equilibration buffer, the column was eluted using a step gradient of 10 ml each with 0.4 M, 0.55 M, and 1 M step gradient of KCl in TEG buffer. The fractions that contain most of the SpHst4-His protein (confirmed by SDS-polyacrylamide gel analysis) were pooled and dialyzed with 1 liter of TEG buffer and loaded onto 1-ml DEAE column (GE Health) equilibrated

with TEG buffer. Upon washing with 3 ml of equilibration buffer, the column was eluted with a 20-ml linear gradient of KCl (0.05–0.6 M) in TEG buffer. Most of SpHst4 was found in the flow-through fraction (Fig. S1), which was divided into small aliquots and stored at −80 °C. The SpHst4-His protein was approximately 98% pure (Fig. S1, lane 4), and its concentration was determined by the Bradford method.

GST pull-down assay

Expression, immobilization of GST fusion constructs, and GST-pull-down assay were similar to the procedures described previously.[45] *E. coli* (BL21Star/DE3) cells (Stratagene) harboring the pGEX4T-SpMyh1 plasmid were cultured in Luria-Bertani broth containing 100 μg/ml ampicillin. Protein expression was induced as described above. The cell extracts from a 0.5-liter culture were immobilized onto glutathione–Sepharose 4B (GE Health). Immobilized GST-SpMyh1 and GST alone GST beads were incubated with 0.5 mg of cell extracts from Hu1500 containing Hus1-Myc overnight at 4 °C. After washing, the pellets were fractionated on a 10% SDS-polyacrylamide gel and transferred onto a nitrocellulose membrane. Western blot analyses were performed with antibody against c-Myc tag (Santa Cruz Biotechnology).

Coimmunoprecipitation

Hu1500 cell extracts (1 mg) were precleared by incubation with protein A–Sepharose (50 μl) in phosphate-buffered saline with protease inhibitors (Sigma-Aldrich) for 4 h at 4 °C. After removal of the beads, the supernatant was mixed with polyclonal SpMyh1 antibody for 16 h at 4 °C. Then, protein A–Sepharose (50 μl) was added to precipitate SpMyh1. After centrifugation at 1000*g*, the supernatant was collected and the pellet was washed. Both the supernatant (10% of total volume) and pellet fractions were resolved on a 10% SDS-polyacrylamide gel. The Myc-tagged SpHst4 that coprecipitated with SpMyh1 was verified by Western blot analysis with antibody against c-Myc (Santa Cruz Biotechnology).

Chromatin immunoprecipitation assay

The ChIP method was performed according to published procedures.[83] Briefly, *S. pombe* cells were grown to log phase, treated with 5 mM H_2O_2 for 30 min, and then recovered for 1 h in fresh YES medium or left untreated. Cells were washed with phosphate-buffered saline and treated with 1% formaldehyde for 15 min at room temperature to cross-link protein–DNA. Chromatin was purified and sonicated to shear the DNA to 0.5–1 kb. Immunoprecipitation was performed with antibodies against SpMyh1 (polyclonal) or c-Myc (Covance, monoclonal 9E10). After cross-link reversal at 65 °C for over 3 h , the DNA was recovered with Qiagen PCR purification kit and used as a template for qPCR reactions. The qPCR reactions contained templates, primers (see Table S2), and PerfeCta SYBR Green SuperMix (Quanta) and were carried out with Roche LightCyler 480 with PCR cycles of 95 °C for 30 s, 55 °C for 30 s, and 70 °C for 1 min. The relative protein enrichment at each site was calculated according to the formula $2^{\Delta Ct - \Delta CtControl}$, in which ΔCt is the difference between the number of cycles required to go above background in input and immunoprecipitant samples. The control is the sample with protein A–Sepharose beads only. qPCR reactions were carried out in duplicate, and ChIP data averaged over more than three independent experiments.

Supplementary materials related to this article can be found online at doi:10.1016/j.jmb.2010.11.037

Acknowledgements

We thank Drs. Susan Forsburg (University of Southern California) and Charles Hoffman (Boston College) for kindly providing the *S. pombe* strains. We are grateful to Dr. David Beach, a Howard Hughes Medical Institute Investigator at Cold Spring Harbor Laboratory, for providing a *S. pombe* cDNA library. We appreciate the critical reading from Dr. Amrita Madabushi and Mr. Randall Gunther. This work was supported by grants (GM35132 and CA78391) from the National Institute of Health to A.L. The Swedish Cancer Society, Swedish Research Council (V.R.), and the Göran Gustafssons Foundation for Research in Natural Sciences and Medicine provided support to K.E.

References

1. Fraga, C. G., Shigenaga, M. K., Park, J. W., Degan, P. & Ames, B. N. (1990). Oxidative damage to DNA during aging: 8-hydroxy-2'-deoxyguanosine in rat organ DNA and urine. *Proc. Natl Acad. Sci. USA*, **87**, 4533–4537.
2. Lu, A. L., Li, X., Gu, Y., Wright, P. M. & Chang, D. Y. (2001). Repair of oxidative DNA damage. *Cell Biochem. Biophy*, **35**, 141–170.
3. Lu, A. L., Bai, H., Shi, G. & Chang, D. Y. (2006). MutY and MutY homologs (MYH) in genome maintenance. *Front Biosci*, **11**, 3062–3080.
4. Loeb, L. A. & Christians, F. C. (1996). Multiple mutations in human cancers. *Mutat. Res.* **350**, 279–286.
5. Barzilai, A. & Yamamoto, K. (2004). DNA damage responses to oxidative stress. *DNA Repair (Amst)*, **3**, 1109–1115.
6. Krokan, H. E., Nilsen, H., Skorpen, F., Otterlei, M. & Slupphaug, G. (2000). Base excision repair of DNA in mammalian cells. *FEBS Lett.* **476**, 73–77.
7. Hitomi, K., Iwai, S. & Tainer, J. A. (2007). The intricate structural chemistry of base excision repair machinery: implications for DNA damage recognition, removal, and repair. *DNA Repair (Amst)*, **6**, 410–428.
8. Mol, C. D., Parikh, S. S., Putnam, C. D., Lo, T. P. & Tainer, J. A. (1999). DNA repair mechanisms for the recognition and removal of damaged DNA bases. *Annu. Rev. Biophys. Biomol. Struct.* **28**, 101–128.
9. Memisoglu, A. & Samson, L. (2000). Base excision repair in yeast and mammals. *Mutat. Res.* **451**, 39–51.

10. Michaels, M. L. & Miller, J. H. (1992). The GO system protects organisms from the mutagenic effect of the spontaneous lesion 8-hydroxyguanine (7,8-dihydro-8-oxo-guanine). *J. Bacteriol.* **174**, 6321–6325.
11. Tchou, J. & Grollman, A. P. (1993). Repair of DNA containing the oxidatively-damaged base 8-hydroxyguanine. *Mutat. Res.* **299**, 277–287.
12. Chang, D. Y., Gu, Y. & Lu, A. L. (2001). Fission yeast (*Schizosaccharomyces pombe*) cells defective in the MutY-homologous glycosylase activity have a mutator phenotype and are sensitive to hydrogen peroxide. *Mol. Genet. Genomics*, **266**, 336–342.
13. Lu, A. L. & Fawcett, W. P. (1998). Characterization of the recombinant MutY homolog, an adenine DNA glycosylase, from *Schizosacchromyces pombe*. *J. Biol. Chem.* **273**, 25098–25105.
14. Al Tassan, N., Chmiel, N. H., Maynard, J., Fleming, N., Livingston, A. L., Williams, G. T. *et al.* (2002). Inherited variants of MYH associated with somatic G:C to T:A mutations in colorectal tumors. *Nat. Genet.* **30**, 227–232.
15. Halford, S. E., Rowan, A. J., Lipton, L., Sieber, O. M., Pack, K., Thomas, H. J. *et al.* (2003). Germline mutations but not somatic changes at the MYH locus contribute to the pathogenesis of unselected colorectal cancers. *Am. J. Pathol.* **162**, 1545–1548.
16. Jones, S., Emmerson, P., Maynard, J., Best, J. M., Jordan, S., Williams, G. T. *et al.* (2002). Biallelic germline mutations in MYH predispose to multiple colorectal adenoma and somatic G:C→T:A mutations. *Hum. Mol. Genet.* **11**, 2961–2967.
17. Sieber, O. M., Lipton, L., Crabtree, M., Heinimann, K., Fidalgo, P., Phillips, R. K. *et al.* (2003). Multiple colorectal adenomas, classic adenomatous polyposis, and germ-line mutations in MYH. *N. Engl. J. Med.* **348**, 791–799.
18. Sampson, J. R., Dolwani, S., Jones, S., Eccles, D., Ellis, A., Evans, D. G. *et al.* (2003). Autosomal recessive colorectal adenomatous polyposis due to inherited mutations of MYH. *Lancet*, **362**, 39–41.
19. Dali-Youcef, N., Lagouge, M., Froelich, S., Koehl, C., Schoonjans, K. & Auwerx, J. (2007). Sirtuins: the 'magnificent seven', function, metabolism and longevity. *Ann. Med.* **39**, 335–345.
20. Michan, S. & Sinclair, D. (2007). Sirtuins in mammals: insights into their biological function. *Biochem. J.* **404**, 1–13.
21. Blander, G. & Guarente, L. (2004). The Sir2 family of protein deacetylases. *Annu. Rev. Biochem.* **73**, 417–435.
22. Brachmann, C. B., Sherman, J. M., Devine, S. E., Cameron, E. E., Pillus, L. & Boeke, J. D. (1995). The SIR2 gene family, conserved from bacteria to humans, functions in silencing, cell cycle progression, and chromosome stability. *Genes Dev.* **9**, 2888–2902.
23. Lavu, S., Boss, O., Elliott, P. J. & Lambert, P. D. (2008). Sirtuins—novel therapeutic targets to treat age-associated diseases. *Nat. Rev. Drug Discov.* **7**, 841–853.
24. Haldar, D. & Kamakaka, R. T. (2008). Fission yeast Hst4 functions in DNA damage response by regulating histone H3 K56 acetylation. *Eukaryot. Cell*, **7**, 800–813.
25. Durand-Dubief, M., Sinha, I., Fagerstrom-Billai, F., Bonilla, C., Wright, A., Grunstein, M. & Ekwall, K. (2007). Specific functions for the fission yeast Sirtuins Hst2 and Hst4 in gene regulation and retrotransposon silencing. *EMBO J*, **26**, 2477–2488.
26. Chen, C. C., Carson, J. J., Feser, J., Tamburini, B., Zabaronick, S., Linger, J. & Tyler, J. K. (2008). Acetylated lysine 56 on histone H3 drives chromatin assembly after repair and signals for the completion of repair. *Cell*, **134**, 231–243.
27. Li, Q., Zhou, H., Wurtele, H., Davies, B., Horazdovsky, B., Verreault, A. & Zhang, Z. (2008). Acetylation of histone H3 lysine 56 regulates replication-coupled nucleosome assembly. *Cell*, **134**, 244–255.
28. Ozdemir, A., Masumoto, H., Fitzjohn, P., Verreault, A. & Logie, C. (2006). Histone H3 lysine 56 acetylation: a new twist in the chromosome cycle. *Cell Cycle*, **5**, 2602–2608.
29. Freeman-Cook, L. L., Sherman, J. M., Brachmann, C. B., Allshire, R. C., Boeke, J. D. & Pillus, L. (1999). The *Schizosaccharomyces pombe* hst4(+) gene is a SIR2 homologue with silencing and centromeric functions. *Mol. Biol. Cell*, **10**, 3171–3186.
30. Bartek, J., Lukas, C. & Lukas, J. (2004). Checking on DNA damage in S phase. *Nat. Rev. Mol. Cell Biol.* **5**, 792–804.
31. Sancar, A., Lindsey-Boltz, L. A., Unsal-Kacmaz, K. & Linn, S. (2004). Molecular mechanisms of mammalian DNA repair and the DNA damage checkpoints. *Annu. Rev. Biochem*, **73**, 39–85.
32. Ehrenhofer-Murray, A. E. (2004). Chromatin dynamics at DNA replication, transcription and repair. *Eur. J. Biochem.* **271**, 2335–2349.
33. Canman, C. E. (2001). Replication checkpoint: Preventing mitotic catastrophe. *Curr. Biol.* **11**, R121–R124.
34. Longhese, M. P., Foiani, M., Muzi-Falconi, M., Lucchini, G. & Plevani, P. (1998). DNA damage checkpoint in budding yeast. *EMBO J.* **17**, 5525–5528.
35. Zhou, B. B. & Elledge, S. J. (2000). The DNA damage response: putting checkpoints in perspective. *Nature*, **408**, 433–439.
36. Zou, L. & Elledge, S. J. (2003). Sensing DNA damage through ATRIP recognition of RPA–ssDNA complexes. *Science*, **300**, 1542–1548.
37. Hang, H. & Lieberman, H. B. (2000). Physical interactions among human checkpoint control proteins HUS1p, RAD1p, and RAD9p, and implications for the regulation of cell cycle progression. *Genomics*, **65**, 24–33.
38. St Onge, R. P., Udell, C. M., Casselman, R. & Davey, S. (1999). The human G2 checkpoint control protein hRAD9 is a nuclear phosphoprotein that forms complexes with hRAD1 and hHUS1. *Mol. Biol. Cell*, **10**, 1985–1995.
39. Dore, A. S., Kilkenny, M. L., Rzechorzek, N. J. & Pearl, L. H. (2009). Crystal structure of the Rad9-Rad1-Hus1 DNA damage checkpoint complex—implications for clamp loading and regulation. *Mol. Cell*, **34**, 735–745.
40. Sohn, S. Y. & Cho, Y. (2009). Crystal structure of the human Rad9-Hus1-Rad1 clamp. *J. Mol. Biol.* **390**, 490–502.
41. Xu, M., Bai, L., Gong, Y., Xie, W., Hang, H. & Jiang, T. (2009). Structure and functional implications of the human Rad9-Hus1-Rad1 cell cycle checkpoint complex. *J. Biol. Chem.* **284**, 20457–20461.
42. Burtelow, M. A., Roos-Mattjus, P. M., Rauen, M., Babendure, J. R. & Karnitz, L. M. (2001). Reconstitution

and molecular analysis of the hRad9-hHus1-hRad1 (9-1-1) DNA damage responsive checkpoint complex. *J. Biol. Chem.* **276**, 25903–25909.
43. Shiomi, Y., Shinozaki, A., Nakada, D., Sugimoto, K., Usukura, J., Obuse, C. & Tsurimoto, T. (2002). Clamp and clamp loader structures of the human checkpoint protein complexes, Rad9-Rad1-Hus1 and Rad17-RFC. *Genes Cells*, **7**, 861–868.
44. Venclovas, C. & Thelen, M. P. (2000). Structure-based predictions of Rad1, Rad9, Hus1 and Rad17 participation in sliding clamp and clamp-loading complexes. *Nucleic Acids Res.* **28**, 2481–2493.
45. Chang, D. Y. & Lu, A. L. (2005). Interaction of checkpoint proteins Hus1/Rad1/Rad9 with DNA base excision repair enzyme MutY homolog in fission yeast, *Schizosaccharomyces pombe*. *J. Biol. Chem.* **280**, 408–417.
46. Shi, G., Chang, D. Y., Cheng, C. C., Guan, X., Venclovas, C. & Lu, A. L. (2006). Physical and functional interactions between MutY homolog (MYH) and checkpoint proteins Rad9-Rad1-Hus1. *Biochem. J.* **400**, 53–62.
47. Fernandez-Capetillo, O. & Nussenzweig, A. (2004). Linking histone deacetylation with the repair of DNA breaks. *Proc. Natl Acad. Sci. USA*, **101**, 1427–1428.
48. Iizuka, M. & Smith, M. M. (2003). Functional consequences of histone modifications. *Curr. Opin. Genet. Dev.* **13**, 154–160.
49. Bjerling, P., Silverstein, R. A., Thon, G., Caudy, A., Grewal, S. & Ekwall, K. (2002). Functional divergence between histone deacetylases in fission yeast by distinct cellular localization and *in vivo* specificity. *Mol. Cell Biol.* **22**, 2170–2181.
50. Freeman-Cook, L. L., Gomez, E. B., Spedale, E. J., Marlett, J., Forsburg, S. L., Pillus, L. & Laurenson, P. (2005). Conserved locus-specific silencing functions of *Schizosaccharomyces pombe* sir2+. *Genetics*, **169**, 1243–1260.
51. Redon, C., Pilch, D., Rogakou, E., Sedelnikova, O., Newrock, K. & Bonner, W. (2002). Histone H2A variants H2AX and H2AZ. *Curr. Opin. Genet. Dev.* **12**, 162–169.
52. Nakamura, T. M., Du, L. L., Redon, C. & Russell, P. (2004). Histone H2A phosphorylation controls Crb2 recruitment at DNA breaks, maintains checkpoint arrest, and influences DNA repair in fission yeast. *Mol. Cell Biol.* **24**, 6215–6230.
53. Paull, T. T., Rogakou, E. P., Yamazaki, V., Kirchgessner, C. U., Gellert, M. & Bonner, W. M. (2000). A critical role for histone H2AX in recruitment of repair factors to nuclear foci after DNA damage. *Curr. Biol.* **10**, 886–895.
54. Wright, W. E. & Shay, J. W. (2005). Telomere-binding factors and general DNA repair. *Nat. Genet.* **37**, 116–118.
55. Muftuoglu, M., Wong, H. K., Imam, S. Z., Wilson, D. M., III, Bohr, V. A. & Opresko, P. L. (2006). Telomere repeat binding factor 2 interacts with base excision repair proteins and stimulates DNA synthesis by DNA polymerase beta. *Cancer Res.* **66**, 113–124.
56. Wang, Z., Rhee, D. B., Lu, J., Bohr, C. T., Zhou, F., Vallabhaneni, H. *et al.* (2010). Characterization of oxidative guanine damage and repair in mammalian telomeres. *PLoS. Genet.* **6**, e1000951.
57. Sanchez, J. A., Kim, S. M. & Huberman, J. A. (1998). Ribosomal DNA replication in the fission yeast, *Schizosaccharomyces pombe*. *Exp. Cell Res.* **238**, 220–230.
58. Khair, L., Chang, Y. T., Subramanian, L., Russell, P. & Nakamura, T. M. (2010). Roles of the checkpoint sensor clamp Rad9-Rad1-Hus1 (911)-complex and the clamp loaders Rad17-RFC and Ctf18-RFC in *Schizosaccharomyces pombe* telomere maintenance. *Cell Cycle, 9.*
59. Nakamura, T. M., Moser, B. A. & Russell, P. (2002). Telomere binding of checkpoint sensor and DNA repair proteins contributes to maintenance of functional fission yeast telomeres. *Genetics*, **161**, 1437–1452.
60. Schwer, B. & Verdin, E. (2008). Conserved metabolic regulatory functions of sirtuins. *Cell Metab.* **7**, 104–112.
61. Lombard, D. B., Schwer, B., Alt, F. W. & Mostoslavsky, R. (2008). SIRT6 in DNA repair, metabolism and ageing. *J. Intern. Med.* **263**, 128–141.
62. Mostoslavsky, R., Chua, K. F., Lombard, D. B., Pang, W. W., Fischer, M. R., Gellon, L. *et al.* (2006). Genomic instability and aging-like phenotype in the absence of mammalian SIRT6. *Cell*, **124**, 315–329.
63. Michishita, E., McCord, R. A., Berber, E., Kioi, M., Padilla-Nash, H., Damian, M. *et al.* (2008). SIRT6 is a histone H3 lysine 9 deacetylase that modulates telomeric chromatin. *Nature*, **452**, 492–496.
64. Michishita, E., McCord, R. A., Boxer, L. D., Barber, M. F., Hong, T., Gozani, O. & Chua, K. F. (2009). Cell cycle-dependent deacetylation of telomeric histone H3 lysine K56 by human SIRT6. *Cell Cycle*, **8**, 2664–2666.
65. Yang, B., Zwaans, B. M., Eckersdorff, M. & Lombard, D. B. (2009). The sirtuin SIRT6 deacetylates H3 K56Ac *in vivo* to promote genomic stability. *Cell Cycle*, **8**, 2662–2663.
66. Oikawa, S. & Kawanishi, S. (1999). Site-specific DNA damage at GGG sequence by oxidative stress may accelerate telomere shortening. *FEBS Lett.* **453**, 365–368.
67. Rubio, M. A., Davalos, A. R. & Campisi, J. (2004). Telomere length mediates the effects of telomerase on the cellular response to genotoxic stress. *Exp. Cell Res.* **298**, 17–27.
68. von Zglinicki, T. (2002). Oxidative stress shortens telomeres. *Trends Biochem. Sci.* **27**, 339–344.
69. Opresko, P. L., Fan, J., Danzy, S., Wilson, D. M., III & Bohr, V. A. (2005). Oxidative damage in telomeric DNA disrupts recognition by TRF1 and TRF2. *Nucleic Acids Res.* **33**, 1230–1239.
70. Celic, I., Masumoto, H., Griffith, W. P., Meluh, P., Cotter, R. J., Boeke, J. D. & Verreault, A. (2006). The sirtuins Hst3 and Hst4p preserve genome integrity by controlling histone H3 lysine 56 deacetylation. *Curr. Biol.* **16**, 1280–1289.
71. Lamming, D. W., Latorre-Esteves, M., Medvedik, O., Wong, S. N., Tsang, F. A., Wang, C. *et al.* (2005). HST2 mediates SIR2-independent life-span extension by calorie restriction. *Science*, **309**, 1861–1864.
72. Maas, N. L., Miller, K. M., DeFazio, L. G. & Toczyski, D. P. (2006). Cell cycle and checkpoint regulation of histone H3 K56 acetylation by Hst3 and Hst4. *Mol. Cell*, **23**, 109–119.
73. Thaminy, S., Newcomb, B., Kim, J., Gatbonton, T., Foss, E., Simon, J. & Bedalov, A. (2007). Hst3 is

regulated by Mec1-dependent proteolysis and controls the S phase checkpoint and sister chromatid cohesion by deacetylating histone H3 at lysine 56. *J. Biol. Chem.* **282**, 37805–37814.
74. Xhemalce, B., Miller, K. M., Driscoll, R., Masumoto, H., Jackson, S. P., Kouzarides, T. *et al*. (2007). Regulation of histone H3 lysine 56 acetylation in *Schizosaccharomyces pombe*. *J. Biol. Chem.* **282**, 15040–15047.
75. Chen, C. C., Carson, J. J., Feser, J., Tamburini, B., Zabaronick, S., Linger, J. & Tyler, J. K. (2008). Acetylated lysine 56 on histone H3 drives chromatin assembly after repair and signals for the completion of repair. *Cell*, **134**, 231–243.
76. Li, Q., Zhou, H., Wurtele, H., Davies, B., Horazdovsky, B., Verreault, A. & Zhang, Z. (2008). Acetylation of histone H3 lysine 56 regulates replication-coupled nucleosome assembly. *Cell*, **134**, 244–255.
77. Masumoto, H., Hawke, D., Kobayashi, R. & Verreault, A. (2005). A role for cell-cycle-regulated histone H3 lysine 56 acetylation in the DNA damage response. *Nature*, **436**, 294–298.
78. Chang, D. Y. & Lu, A. L. (2002). Functional interaction of MutY homolog (MYH) with proliferating cell nuclear antigen (PCNA) in fission yeast, *Schizosaccharomyces pombe*. *J. Biol. Chem.* **277**, 11853–11858.
79. Celic, I., Verreault, A. & Boeke, J. D. (2008). Histone H3 K56 hyperacetylation perturbs replisomes and causes DNA damage. *Genetics*, **179**, 1769–1784.
80. Moreno, S., Klar, A. & Nurse, P. (1991). Molecular genetic analysis of fission yeast *Schizosaccharomyces pombe*. *Methods Enzymol.* **194**, 795–823.
81. Bahler, J., Wu, J. Q., Longtine, M. S., Shah, N. G., McKenzie, A., III, Steever, A. B. *et al.* (1998). Heterologous modules for efficient and versatile PCR-based gene targeting in *Schizosaccharomyces pombe*. *Yeast*, **14**, 943–951.
82. Ausubel, F. M., Brent, R., Kingston, R. E., Moore, D. D., Seidman, J. G., Smith, J. A. & Struhl, K. (1994). *Current Protocols in Molecular Biology*. John Wiley & Sons, New York, NY.
83. Ampatzidou, E., Irmisch, A., O'Connell, M. J. & Murray, J. M. (2006). Smc5/6 is required for repair at collapsed replication forks. *Mol. Cell Biol.* **26**, 9387–9401.